EPJ Web of Conferences **20**, 02007 (2012)
DOI: 10.1051/epjconf/20122002007

Role of Resonances in the Electromagnetic Production of Kaon Near Threshold

T. Mart[a]

Departemen Fisika, FMIPA, Universitas Indonesia, Depok 16424, Indonesia

Abstract. Kaon photo- and electroproduction processes near their production thresholds are investigated by using an effective Lagrangian method. It is found that the nucleon and hyperon resonances play a considerably important role in this kinematics. It is also found that kaon photoproduction off the proton may provide a new arena for investigating the existence of the narrow resonance predicted by the soliton models.

1 Introduction

There is a number of strong arguments which supports kaon photoproduction as an important tool for investigating the evidence and properties of resonances. One of them is that not all resonances predicted by the constituent quark models have significant decay widths to the πN channels [1], the main reactions used by the Particle Data Group [2] to extract the properties of resonances as well as to determine their existence. According to the constituent quark models some resonances may mostly decay to the ηN or KY channels. Due to the explicit presence of the strangeness in the final states, the latter is of special interest. For instance, the existence of a new "missing" resonance $D_{13}(1895)$, which had been previously predicted by a certain quark model to have a substantially large branching fraction to the strangeness channel, was reported in the phenomenological study of the $K^+\Lambda$ photoproduction [3]. On the other hand, the extracted elementary operator can be further used to study the production of hypernuclei [4]. However, compared to the πN channels this additional degree of freedom leads to more uncertainties in the $K\Lambda$ and $K\Sigma$ channels. Therefore, more intensive theoretical and experimental studies on the electromagnetic production of kaon are inevitable to overcome this drawback.

There have been considerable efforts to this end in the last decades. Most studies have been performed in the framework of an effective Lagrangian approach, which have obvious advantages, i.e. relatively simple and can be directly compared with experimental data obtained or extracted from various processes. Other studies are based on the chiral quark model and multipoles approach. In spite of significant progress achieved in both theoretical and experimental aspects, there are several unsolved problems that need serious attention. For a brief review on this topic we refer the reader to Ref. [5].

On the experimental side, the advancements in the detector and accelerator technologies in the last decade have led to a huge number of new experimental data with high statistics [6]. At present, even double polarization observables, such as C_x, C_z, $O_{x'}$, and $O_{z'}$, can be measured with high accuracy. Obviously, this achievement paves the way to study the role of nucleon, hyperon, and kaon resonances in the photoproduction process in a more precise fashion.

In this paper we intend to discuss the effects of nucleon and hyperon resonances in both photo- and electroproduction of kaon. There are six isospin channels available. However, in view of the availability of experimental data, we will focus our discussion on the $K^+\Lambda$ and $K^0\Lambda$ channels, as well as the $K^+\Sigma^0$ channel. To study the minimum effect of resonances, it is important to focus our attention to the threshold region, since at this kinematics the effect of higher lying resonances can be effectively minimized.

[a] e-mail: tmart@fisika.ui.ac.id

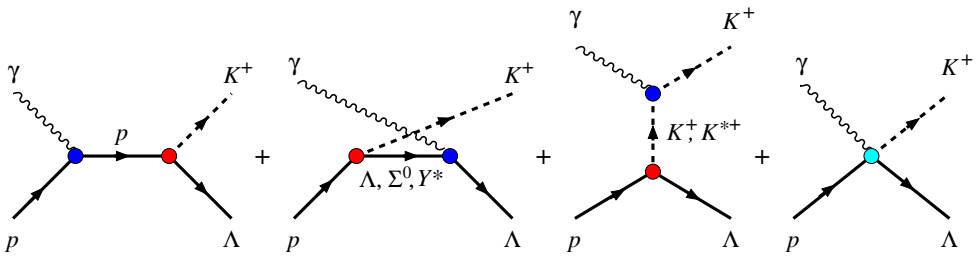

Fig. 1. Feynman diagrams of the background amplitude.

2 Photo- and Electroproduction of the $K^+\Lambda$

The photo- or electroproduction process of $K^+\Lambda$ can be considered as the real or virtual photon production

$$\gamma_{\mathrm{r,v}}(k) + p(p_p) \rightarrow K^+(q_K) + \Lambda(p_\Lambda)\,. \tag{1}$$

In the effective Lagrangian approach the background terms of this process can be parametrized by using a series of tree-level Feynman diagrams shown in Fig. 1. They consist of the standard s-, u-, and t-channel Born terms along with the $K^{*+}(892)$ and $K_1(1270)$ t-channel vector mesons. Since we consider the photoproduction near threshold, we would expect that no hadronic form factors is required in all hadronic vertices of the diagrams in Fig. 1. This has the advantage that we can further limit the number of free parameters as well as uncertainties in our model. Furthermore, as shown by Ref. [7], the use of hadronic form factor could lead to an underprediction of differential cross section data at forward angles.

By limiting the energy range of interest from threshold up to 50 MeV above the threshold, there are 139 experimental data points in the database, consisting of 115 differential cross sections, 18 recoil polarizations, and 6 photon beam asymmetries. In addition, there are 18 data points of beam-recoil double polarizations, O_x and O_z, and target asymmetry T from the latest GRAAL measurement. The energy limitation of the process leads to the fact that only the resonance state $S_{11}(1650)$ contributes to the process. As a consequence only the resonant electric multipole E_{0+} amplitude exists and the resonance contribution is extremely simplified.

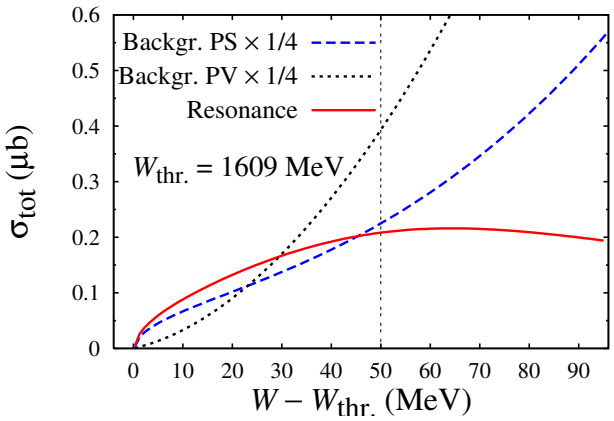

Fig. 2. Contribution of the background terms and the $S_{11}(1650)$ resonance amplitudes to the total cross section for the PS and PV couplings. Note that contribution of the $S_{11}(1650)$ resonance is the same in both couplings. The vertical line at 50 MeV above the production threshold indicates the upper limit of the energy of the analysis [8].

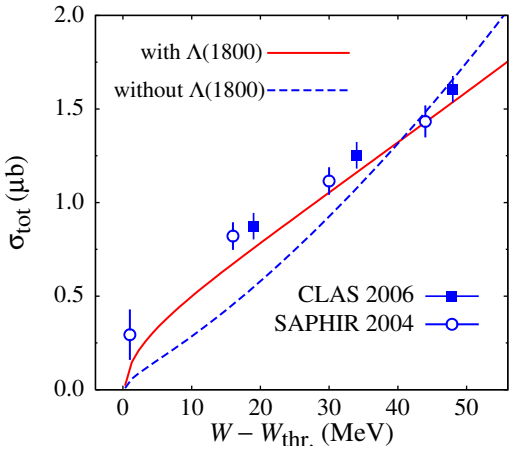

Fig. 3. The hyperon resonance $S_{01}(1800)$ effect on the total cross sections in the PS model [8].

Comparison between contribution of this resonance with contributions of the backgrounds in the pseudoscalar (PS) and pseudovector (PV) models to the total cross section is shown in Fig. 2. It is found that the $S_{11}(1650)$ contributes more than 20% to the total cross section in the PS model. In the PV model its contribution varies from about 15% up to 70%, depending on the energy. In Ref. [13] it is shown that this resonance is only significant in the model that fits to the SAPHIR data, in which around 20% of the total cross section comes from the contribution of this resonance. We also note that the background contribution of PV model starts to substantially increase at $W = 25$ MeV above the threshold, as shown in Fig. 2. This indicates the deficiency of the PV model at higher energies. In previous analyses it was found that the deficiency of the PV model is caused by the fact that its background terms are found to be too large compared to those of the PS model. The result shown here is therefore consistent with previous analyses. Furthermore, from Fig. 2 it is apparent that between threshold and $W = 25$ MeV the PV background terms yield smaller contribution to the cross section. Thus, very close to threshold the use of SU(3) main coupling constants is also acceptable in the PV model.

It is also found that significant improvement in the χ^2 could be obtained if the $S_{01}(1800)$ hyperon resonance is included in the process. This result corroborates the finding of Janssen *et al.* [14], since the large hadronic cut-off requires another mechanism to damp the cross section at high energies. This is achieved by a destructive interference between the hyperon resonance contribution and other background terms. Such an interference is also observed in the present work, as obviously indicated by the total cross sections in Fig. 3. Although underpredicts experimental data at $W - W_{\rm thr} < 40$ MeV, the model that excludes the $S_{01}(1800)$ resonance starts to overpredict the data, and therefore starts to diverge, at $W - W_{\rm thr} > 40$ MeV.

The improvement obtained by including this resonance is not only observed in the total as well as differential cross sections, but also found in the calculated recoil polarizations and the target asymmetry [8]. It is also found that including this hyperon resonance results in a perfect agreement between the PS model and experimental data, especially the SAPHIR and GRAAL ones.

Note that the result shown here is obtained by including also the electroproduction data. More detailed information on this topic can be found in Ref. [8].

3 Photo- and Electroproduction of the $K^0\Lambda$

Recently, the Tohoku group has experimentally studied photoproduction of the neutral kaon on a deuteron via the inclusive $d(\gamma, K^0)YN$ process [9]. The result implies that the elementary operator of the $\gamma + p \rightarrow K^+ + \Lambda$ process plays an important role in the production on the deuteron. As a consequence, a more detailed study of the K^0 elementary production is urgently required. There are two

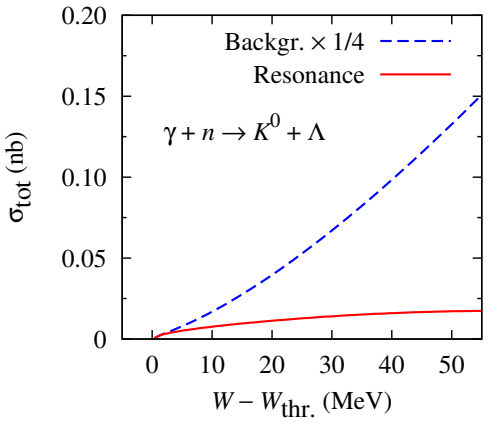

Fig. 4. Contribution of the background terms and the $S_{11}(1650)$ resonance amplitude to the total cross section of the $\gamma + n \to K^0 + \Lambda$ channel [10].

possibilities to approach this case. The first possibility is to extract the elementary operator from the deuteron data by utilizing the already known elementary operator. The second is by directly extend the $K^+\Lambda$ channel calculation to the $K^0\Lambda$ channel.

Since the effective Lagrangian model described in the previous Section can be easily extended to the $K^0\Lambda$ isospin channel, we will describe this approach in this paper. For this purpose to relate the hadronic coupling constants of the background terms in the two channels we can employ the SU(3) symmetry, i.e.,

$$g_{K^+\Lambda p} = g_{K^0\Lambda n},\ g_{K^+\Sigma^0 p} = -g_{K^0\Sigma^0 n},\ g^{V,T}_{K^{*+}\Lambda p} = g^{V,T}_{K^{*0}\Lambda n}. \tag{2}$$

In the $K^0\Lambda$ production the vector meson exchanged in the t-channel is the $K^{*0}(896.10)$. Therefore, the transition moment in K^+ production, $g_{K^*K\gamma}$, must be replaced by the neutral transition moment by using [11]

$$g_{K^{*0}K^0\gamma}/g_{K^{*+}K^+\gamma} = -1.53 \pm 0.20\,. \tag{3}$$

Since in the case of the $K_1(1270)$ vector meson exchange, there is no sufficient information from the Particle Data Book [2], we use the value given by the Kaon-Maid [12],

$$r_{K_1K\gamma} \equiv g_{K_1^0K^0\gamma}/g_{K_1^+K^+\gamma} = -0.45\,, \tag{4}$$

which was extracted from simultaneous fitting of the $K^+\Sigma^0$ and $K^0\Sigma^+$ photoproduction data. The $S_{01}(1800)$ u-channel stays unmodified, since from Eq. (2) we have $g_{K^+\Lambda p} = g_{K^0\Lambda n}$, whereas the electromagnetic vertex $\gamma Y^{*0}\Lambda$ in both $K^+\Lambda$ and $K^0\Lambda$ channels is the same.

In the resonance term we have to replace the helicity photon couplings of the proton $A^p_{1/2}$ with that of the neutron, where [2]

$$A^n_{1/2} = -0.015 \pm 0.021\ \text{GeV}^{-1/2}\,. \tag{5}$$

Note that this coupling is substantially smaller than the proton coupling, i.e. $A^p_{1/2} = 0.053 \pm 0.016$ $\text{GeV}^{-1/2}$ [2]. As a consequence, we may expect a relatively smaller resonance contribution in the case of $K^0\Lambda$ production. This is confirmed by Fig. 4, where we compare the background and resonance contributions to the total cross section of the $K^+\Lambda$ and $K^0\Lambda$ photoproduction. Different from the $K^+\Lambda$ channel, in which contribution of the $S_{11}(1650)$ resonance is more or less 20% (in the PS coupling), contribution of this resonance to the $K^0\Lambda$ total cross section at $W = 50$ MeV above threshold is only about 3%.

In Ref. [10] it is also shown that the elementary operator for electroproduction can be utilized to explore the effect of the K^0 charge distribution.

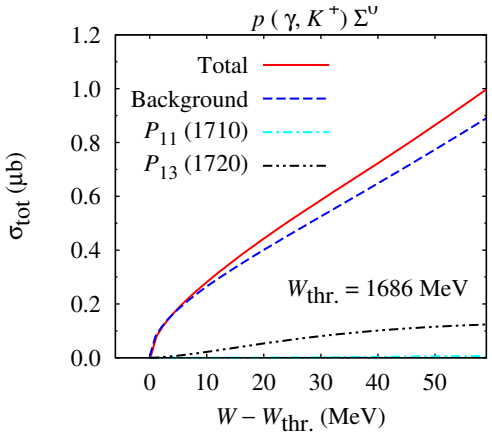

Fig. 5. Contribution of the background terms as well as the $P_{11}(1710)$- and $P_{13}(1720)$-resonance amplitudes to the total cross section of the $\gamma + p \to K^+ + \Sigma^0$ channel.

4 Photo- and Electroproduction of the $K^+\Sigma^0$

Due to the higher mass of the Σ^0 compared to the Λ, the threshold energy of the $K^+\Sigma^0$ channel is about 80 MeV higher than that of the $K^+\Lambda$ channel (i.e. 1686 MeV). As a consequence, more nucleon resonances can participate to the process, whereas the $S_{11}(1650)$ MeV lies below the threshold and therefore is excluded from our list since in the resonance formulation used in this analysis the inclusion of resonances below the threshold is not possible.

In the energy range from threshold up to 50 MeV above (i.e. 1736 MeV) there are two well known nucleon resonances, namely the $P_{11}(1710)$ and $P_{13}(1720)$ states. Their contributions to the total cross section of the $\gamma + p \to K^+ + \Sigma^0$ channel are shown in Fig. 5, where the background terms contribution along with the total contribution are shown for comparison. It is clear from this figure that the role of the $P_{13}(1720)$ state is more important than that of the $P_{11}(1710)$ state. This finding is consistent with the finding of Ref. [13]. Further study of the $K^+\Sigma^0$ and related channels is in progress.

5 Extending the Analysis to 1730 MeV

The energy coverage of the phenomenological models presented in the previous Sections should be extended for the investigation of the narrow resonance predicted by the soliton models [15,16]. The soliton models predict a P_{11} ($J^p = 1/2^+$) narrow resonance as a non-strange partner of the well known pentaquark with the mass between 1650 and 1690 MeV. The model presented in the previous Sections can describe experimental data only up to 1660 MeV. Therefore, the model should be extended up to 1730 MeV, at least, since in order to investigate this narrow state we have to scan its mass around the predicted mass [17]. The extension has been discussed in Ref. [18], where five more nucleon resonances listed in Table 1 has been included, along with the $S_{11}(1650)$ resonance which has been used in the previous model.

To investigate the model dependence, two phenomenological models are proposed in this study. In the first model (Model 1) the maximum variation of the photon amplitudes during the fitting process is constrained within 10% of the original PDG values. In the second model (Model 2) the variation of the resonance parameters is not constrained as strict as in Model 1, i.e., all parameters are allowed to vary within the PDG error bars.

Contribution of the background and resonance terms in the two models are shown in Fig. 6. It is found that the characteristic of resonance contributions can be comprehended from the values of kaon branching ratio β_K and photon helicity amplitudes $A_{1/2}$ and $A_{3/2}$ extracted from the fits. The two models show the same dominance of the background terms and the same large contribution of the

Table 1. Properties of the nucleon resonances taken from the Review of Particle Properties [2].

Resonance	M_R (MeV)	Γ_R (MeV)	β_K	$A_{1/2}(p)$ (10^{-3}GeV$^{-1/2}$)	$A_{3/2}(p)$ (10^{-3}GeV$^{-1/2}$)	Overall status
$S_{11}(1650)$	1655^{+15}_{-10}	165 ± 20	0.029 ± 0.004	$+53 \pm 16$	-	****
$D_{15}(1675)$	1675 ± 5	150^{+15}_{-20}	< 0.01	$+19 \pm 8$	$+15 \pm 9$	****
$F_{15}(1680)$	1685 ± 5	130 ± 10	-	-15 ± 6	$+133 \pm 12$	****
$D_{13}(1700)$	1700 ± 50	100 ± 50	< 0.03	-18 ± 13	-2 ± 24	***
$P_{11}(1710)$	1710 ± 30	100^{+150}_{-50}	0.15 ± 0.10	$+9 \pm 22$	-	***
$P_{13}(1720)$	1720^{+30}_{-20}	200^{+100}_{-50}	0.044 ± 0.004	$+18 \pm 30$	-19 ± 20	****

$S_{11}(1650)$ resonance. The differences between them appear at relatively higher energies. The background contribution of Model 2 is somewhat suppressed at this kinematics in order to compensate contributions of the $S_{11}(1650)$, $P_{11}(1710)$ and $P_{13}(1720)$ resonances that tend to increase. From Fig. 6 it is also seen that the peak of the $S_{11}(1650)$ contribution is shifted to higher energy in Model 2. It is obvious that Model 1 is more consistent with our previous multipole analysis [13], i.e., the $S_{11}(1650)$ resonance contributes significantly, in contrast to the $P_{11}(1710)$.

Both Model 1 and Model 2 are used to investigate the existence of the narrow resonance state predicted by the soliton models [15, 16]. For the sake of simplicity we only display the result of Model 1 in Fig. 7, where the resonance mass is scanned from 1620 to 1730 MeV, and the total width $\Gamma_{\text{tot.}}$ is varied from 1 to 10 MeV with 1 MeV step. We have also investigated the variation of the $K\Lambda$ branching ratio $\Gamma_{K\Lambda}$ and found that the best χ^2 would be obtained if we used $\Gamma_{K\Lambda} = 0.2$ and $\Gamma_{\text{tot.}} = 5$ MeV. We found that the result is practically model independent. If we replace the P_{11} narrow resonance with an S_{11} ($J^p = 1/2^-$) resonance we obtain a similar result as shown in the middle panel of Fig. 7. Obviously the same minimum at $m_{N^*} = 1650$ MeV is retained, but a new one clearly appears at $m_{N^*} = 1680$ MeV. The appearance of the minimum $\Delta\chi^2$ at $m_{N^*} = 1650$ MeV in the left and middle panels of Fig. 7 indicates that a real structure really exists at this energy point. In Ref. [18] it is shown that this structure originates from the recoiled Λ polarization data. Finally, in the right panel of Fig. 7 we show the result if we use a P_{13} state instead of the P_{11} or S_{11}. Here we observe that minimum at 1650 MeV almost vanishes and a clear minimum at 1680 MeV, as in the case of the S_{11}, appears. Besides that, we also observe two weaker minima at 1660 and 1700 MeV. However, the minimum at 1680 MeV is interesting in this case, since the possibility that the structure found in the η photoproduction off a neutron can be explained by a P_{13} resonance has been discussed in Ref. [19]. In fact, the most convincing result with the smallest χ^2 would be obtained if one used a $P_{13}(1685)$ state instead of a P_{11} [19].

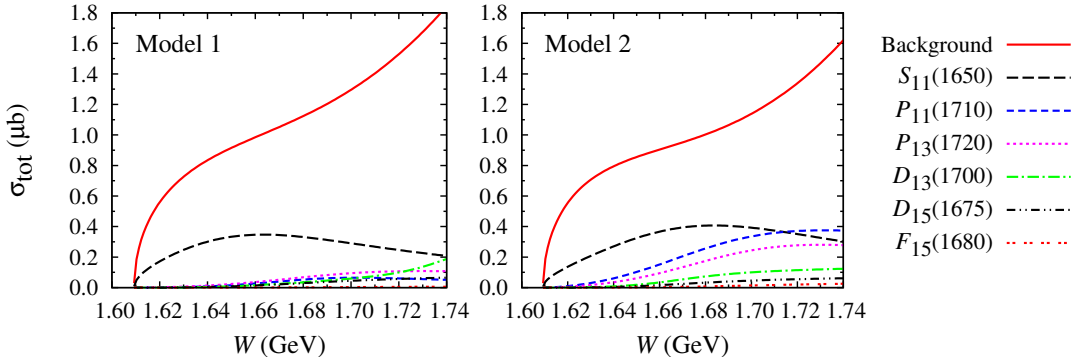

Fig. 6. Contribution of the resonance and background terms to the total cross section for the two models proposed to investigate the P_{11} narrow resonance [18].

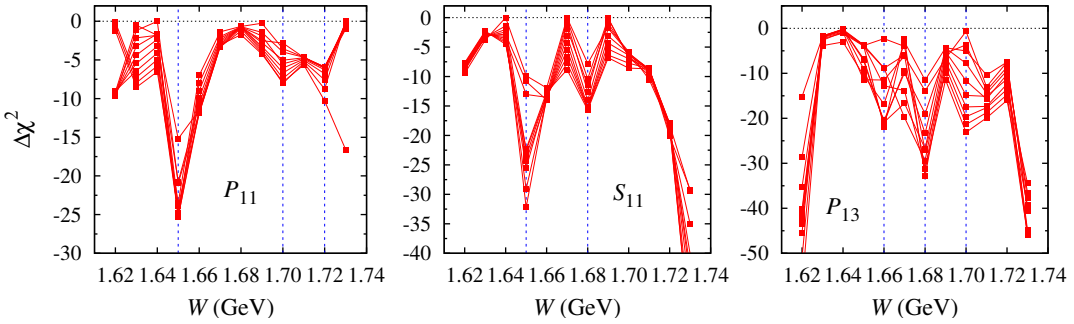

Fig. 7. Change of the χ^2 in the fit of the $K^+\Lambda$ data due to the inclusion of the P_{11} (left panel), S_{11} (middle panel), and P_{13} (right panel) narrow resonances with masses scanned from 1620 to 1730 MeV (step 10 MeV) and $\Gamma_{\text{tot.}}$ taken from 1 to 10 MeV (step 1 MeV) for the $K\Lambda$ branching ratio 0.2. The vertical lines indicate the possible resonance masses [18].

The same minima at $W = 1650$ MeV obtained in fits with S_{11} and P_{11} as shown in Fig. 7 could indicate a problem in determining the spin-parity of the narrow resonance found in the present study. However, this problem could be easily solved if we had more precise total cross section data. As shown in Fig. 8 the inclusion of a narrow resonance with $J^p = 1/2^-$, i.e., the S_{11}, results in a clear dip in the total cross section. Although the appearance of such a dip seems to be unlikely in the $K^+\Lambda$ total cross section, more precise experiments to determine the total cross section would be very helpful to solve this problem.

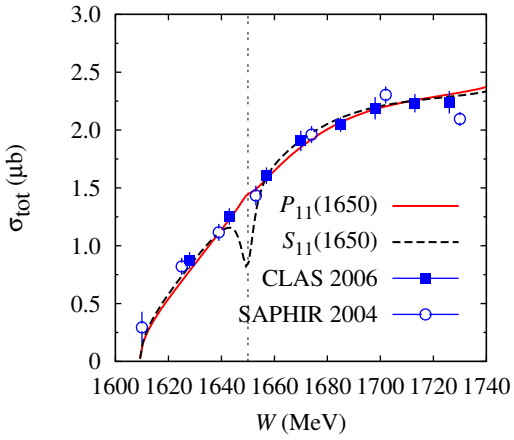

Fig. 8. Effects of the inclusion of P_{11} (solid line) and S_{11} (dashed line) resonances with resonance parameters obtained in the fits of Fig. 7 on the total cross section of the $\gamma + p \to K^+ + \Lambda$ process.

The result obtained in this investigation can be improved if more precise experimental data on the recoiled Λ polarization are available.

6 Conclusion

We have discussed the role of nucleon and hyperon resonances in the kaon photo- and electroproduction processes. It is found that very close to the production threshold the effect of certain resonances is not negligible. In the $K^+\Lambda$ channel the effect of the $S_{11}(1650)$ resonance is found to be around 20%

in the PS model. In the PV model the effect could be larger, depending on the energy. In contrast to this result, the effect is very mild in the $K^0\Lambda$ channel. In the $K^+\Sigma^0$ channel it is found that the effect of the $P_{13}(1720)$ resonance is larger than that of the $P_{11}(1710)$. By extending the model up to 1740 MeV it is concluded that the $S_{11}(1650)$ resonance still plays the most important role in kaon photo- and electroproduction. The effect of the narrow resonance predicted by the soliton model is sizable in the $K^+\Lambda$ channel. As a consequence, kaon photoproduction has opened a new arena for investigating the non-strange partner of the well known pentaquark.

Acknowledgment

The author acknowledges supports from the University of Indonesia and the Competence Grant of the Indonesian Ministry of National Education.

References

1. N. Isgur and G. Karl, Phys. Lett. B **72** (1977) 109; Phys. Rev. D **23** (1981) 817; R. Koniuk and N. Isgur, Phys. Rev. D **21** (1980) 1868; S. Capstick and W. Roberts, Phys. Rev. D **49** (1994) 4570.
2. K. Nakamura *et al.* (Particle Data Group), J. Phys. G **37** (2010) 075021.
3. T. Mart and C. Bennhold, Phys. Rev. C **61** (1999) 012201.
4. B. I. S. van der Ventel, T. Mart, H. F. Lu, H. L. Yadav and G. C. Hillhouse, Annals Phys. **326** (2011) 1085.
5. T. Mart, Int. J. Mod. Phys. E **19** (2010) 2343.
6. M. E. McCracken *et al.*, Phys. Rev. C **81** (2010) 025201 and references therein.
7. P. Bydžovský and T. Mart, Phys. Rev. C **76** (2007) 065202.
8. T. Mart, Phys. Rev. C **82** (2010) 025209.
9. K. Tsukada *et al.*, Phys. Rev. C **78** (2008) 014001.
10. T. Mart, Phys. Rev. C **83** (2011) 048203.
11. T. Mart, C. Bennhold and C. E. Hyde-Wright, Phys. Rev. C **51** (1995) 1074.
12. Available at the Maid homepage http://www.kph.uni-mainz.de/MAID/kaon/kaonmaid.html. The published versions can be found in: Ref. [3]; T. Mart, Phys. Rev. C **62** (2000) 038201; C. Bennhold, H. Haberzettl and T. Mart, arXiv:nucl-th/9909022.
13. T. Mart and A. Sulaksono, Phys. Rev. C **74** (2006) 055203.
14. S. Janssen, J. Ryckebusch, D. Debruyne and T. Van Cauteren, Phys. Rev. C **65** (2001) 015201.
15. D. Diakonov, V. Petrov, and M. Polyakov, Z. Phys. A **359** (1997) 305.
16. H. Walliser and V. B. Kopeliovich, J. Exp. Theor. Phys. **97** (2003) 433 [Zh. Eksp. Teor. Fiz. **124** (2003) 483].
17. R. A. Arndt, Ya. I. Azimov, M. V. Polyakov, I. I. Strakovsky, and R. L. Workman, Phys. Rev. C **69** (2004) 035208.
18. T. Mart, Phys. Rev. D **83** (2011) 094015.
19. V. Kuznetsov *et al.*, Acta Phys. Polon. B **39** (2008) 1949.